VERSITA

Cent. Eur. J. Med. • 5(3) • 2010 • 280-291
DOI: 10.2478/s11536-010-0006-9

Central European Journal of **Medicine**

Aorta transplantation in young apolipoprotein E-deficient mice: Possible model for studies on regression of atherosclerotic lesions?

Research Article

Zbyněk Tonar[1,2,3*], Dagmar Bobková[1], Kirsti Witter[4], Vít Martin Matějka[2], Jana Havlíčková[5], Věra Lánská[6], Rudolf Poledne[1]

[1] *Laboratory for Atherosclerosis Research, Institute for Clinical and Experimental Medicine, Vídeňská 1958/9, 140 21 Prague, Czech Republic*

[2] *Department of Histology and Embryology, Faculty of Medicine in Pilsen, Charles University in Prague, Karlovarská 48, 301 66 Pilsen, Czech Republic*

[3] *Department of Mechanics, Faculty of Applied Sciences, University of West Bohemia, Univerzitní 22, 306 14 Pilsen, Czech Republic*

[4] *Institute of Histology and Embryology, Department of Pathobiology, University of Veterinary Medicine, Veterinärplatz 1, A-1210 Vienna, Austria*

[5] *Laboratory of Pathophysiology of Cardiovascular System, Institute for Clinical and Experimental Medicine, Vídeňská 1958/9, 140 21 Prague, Czech Republic*

[6] *Statistics Unit, Institute for Clinical and Experimental Medicine, Vídeňská 1958/9, 140 21, Prague, Czech Republic*

Received 18 June 2009; Accepted 28 December 2009

Abstract: Syngeneic transplantation of murine aorta segments with advanced atherosclerotic lesions in defined recipients is a valuable model for regression studies. To date, this model has not been used to study the regression of initial atherosclerotic lesions. The aim of this study was to evaluate a microsurgical technique of syngeneic heterotopic transplantation of the thoracic aorta of young apolipoprotein E-deficient (ApoE-/-) mice to the abdominal aorta of wild-type recipients. Stereological quantification methods were tested in order to assess changes in structure and volume of the aortic wall including the involvement of immune cells in changes of the atherosclerotic lesions. The animals were euthanised one month after surgery and histological analysis including stereological quantification of changes in both the grafts and adjacent aorta segments was performed. The overall survival rate of the recipients was 62.5%. No regression of initial atherosclerotic lesion was achieved and neointima formation and elastin degradation prevailed in all transplanted specimens. The volume of the arteriosclerotic lesions was higher ($p<0.001$) and elastin length density was lower ($p<0.001$) in transplanted ApoE-/- samples as compared to adjacent segments. In transplanted grafts, T- and B-lymphocytes, macrophages and neutrophilic granulocytes formed non-random clusters within the vessel wall and they were colocalised with the sutures. The reproducibility of the promising regression model was derogated in young mice by the striking dependence of the results upon the operation technique. Stereological assessment has proven to be accurate, correct and reproducible; it has provided us with robust quantitative estimates, which can be achieved with a reasonable effort.

Keywords: *Heterotopic transplantation • Quantitative histology • Stereology*

* *E-mail: tonar@lfp.cuni.cz*

1. Introduction

Mechanisms of regression of atherosclerotic plaques can be readily studied using the ApoE-deficient mouse model. Apo E-/- mice are characterised by the loss of the ligands for lipoprotein receptors, which is associated with an increase in total cholesterol due to slowed utilisation of remnant-like particles and with an increased risk for the development of atherosclerosis due to low density lipoprotein (LDL) particle accumulation [1-3]. Development of atherosclerotic lesions is also affected by cholesterol reverse transport, in which ApoE plays a pivotal role. Excessive cholesterol is released from the subendothelial space by means of macrophage-derived ApoE [4,5; for review see 6]. Unlike mice and rats with unpertubed cholesterol metabolism, the Apo E-/- mice are characterised by increased cholesterolemia and spontaneous development of atherosclerotic lesions. Basal cholesterolemia of Apo E-/- mice is up to five times higher than that of animals of the same strain without the genetic defect, i.e. approximately 10 mmol/l. Due to the inability of to produce ApoE, ApoE-/- mice are highly sensitive to dietary intervention. In these animals, administration of a cholesterol diet, which mimics increased cholesterol intake by humans in developed countries, leads to an increase in cholesterolaemia and the development of macroscopic atherosclerotic lesions [7]. Sites of predilection and early development of atherosclerosis in the ApoE-/- model include the aortic root and the curvature of the aortic arch and its branches [8].

Lesions developing in the ascendent aorta and aortic arch of ApoE-/- mice are very similar to those in human in both localisation and histological appearance [9,10], although lipoprotein profiles are not the same in both species [11]. In wild-type mice, high density lipoprotein (HDL) represents the majority of lipoprotein particles. In ApoE-/- mice, a shift in advantage of very low LDL (VLDL) and chylomicron remnants can be observed. In contrast, human blood contains predominantly LDL particles [12,13].

Development and regression of atherosclerotic lesions can be readily studied by syngeneic transplantation of cells or vessel segments between ApoE-/- and wild-type animals. Transplantation of macrophages expressing mouse or human apolipoproteins to ApoE-/- recipients can lead to plaque regression or stabilisation with or without the normalisation of the animal's lipoprotein profile [14-17]. Syngeneic transplantation of atherosclerotic aorta segments from ApoE-/- mice to defined recipients seems to be a particularly valuable model for regression studies [18-21]. It was demonstrated that even advanced atherosclerotic lesions can either regress completely in a normolipidaemic environment with normal apolipoprotein levels [18] or at least stabilise and be prevented from progressing in an environment with increased HDL concentration [19]. For reviews on immune mechanisms in development of atherosclerotic lesions, see [22-25].

To date, studies based on the transplantation of aorta segments used only adult animals with fully developed plaques. For examination of subtle regression mechanisms of atherosclerotic lesions it would be, however, desirable to develop a similar transplantation model using young animals. The aim of our study was therefore to evaluate a microsurgical technique of syngeneic heterotopic transplantation of the thoracic aorta in young mice to the abdominal aorta in wild-type recipients as well as to assess and quantify the changes in structure and volume of the aortic wall (preliminarily assessed by [26]), which includes a screening of immune cell involvement in changes of the atherosclerotic lesions.

2. Material and Methods

2.1. Animals and diet

Three-month-old male mice of ApoE-/- (C57Bl/6) strain (n=24) and age-matched syngeneic wild-type mice (n=24) were used. All the animals were obtained from the Jackson Laboratory (Bar Harbor, ME, USA). They weighed 25-30 g at the start of the experiment. Before and after transplantation, the animals were fed a standard laboratory diet (chow), i.e. a 8-mm pelleted diet (SEMED, Prague, Czech Republic) *ad libitum*. Tap water without any pre-treatment was available *ad libitum*. During the experiment, all animals were kept separately in cages (placed in conventional breeding place) on softwood granules as bedding and under standard conditions: fluorescent lighting: approx. 300 lux at 1 m above floor from 07:00 to 18:00, room temperature was controlled at 21 ± 2ºC with 17 air changes per hour and a relative air humidity of 45 ± 5%. The study protocol was approved by the local research ethics committee and the animals were given care according to rules valid in the Czech Republic as well as the European Convention for the Protection of Vertebrate Animals used for Experimental and other Scientific Purposes [27].

Table 1. Primary antibodies.

Antibody	Specifity	Concentration	Company
CD3 monoclonal rabbit anti human (clone SP7)	T-lymphocytes	1:500	LabVision, Fremont, CA, USA
CD20 monoclonal rabbit anti human	B-lymphocytes	1:100	LabVision, Fremont, CA, USA
Monoclonal mouse anti human monocytes/macrophages MCA 874G (clone MAC 387)	Macrophages	1:100	Serotec, Düsseldorf, Germany
purified anti mouse neutrophils rat monoclonal antibody (clone 7/4)	Neutrophilic granulocytes	1:500	AMS Biotechnology Ltd., Abingdon Oxon, UK

2.2. Experimental design

The thoracic aorta of donor mice, which is known to be the site of initiation of atherosclerotic lesions, was transplanted to the abdominal aorta of age-matched syngeneic recipients as follows: from ApoE-/- to ApoE-/- (Group 1, n=8), from ApoE-/- to wild-type (Group 2, n=8), from wild-type to wild-type (Group 3, n=8). Transplanted segments, as well as the segments of donor thoracic aortae situated proximally and distally to the transplanted area, were analysed one month after transplantation.

2.3. Transplantation procedure

The aortic transplantation with infrarenal position was performed as described previously [28]. Donor and recipients were anesthetised by administration of fentanyl and droperidole i. m. (0.5 ml of combination/kg body weight, Innovar-Vet Inj containing 20 mg/ml droperidol + 0.628 mg/ml fentanyl citrate, Janssen, Toronto, Canada) and midazolam (5 mg/kg body weight). Thoracic donor aortae were removed and perfused with chilled heparinised saline; a 5-mm segment was taken from the midportion between the left subclavian artery and diaphragm. Harvested aortae were preserved in chilled saline (-4°C) while the recipient mice were being prepared. The recipient infrarenal aorta was exposed, clamped and transsected. The donor aortic segment was inserted as a tube graft by microsurgical anastomosis (interrupted sutures of 11-0 nylon monofilament, S&T, Neuhausen, Switzerland) as described [18]. The handling time of the transplantation was less than 30 minutes. After removing the aortae, the donors were euthanised by overdose of anaesthesia. The recipient animals were euthanised one month post-surgery by overdose of anaesthesia followed by cervical dislocation with subsequent exsanguination (using decapitation).

2.4. Lipid analysis

After euthanasia, blood (contaminated by a small amount of lymph) was collected in order to analyse plasma cholesterol concentrations. Plasma was harvested by centrifugation of the blood sample (containing 5 μl of 10% EDTA per 1 ml of blood) for 10 minutes at 12,000 rpm. Cholesterol concentrations were measured using colorimetric enzymatic assay kits (Boehringer Mannheim Biochemicals, Germany).

2.5. Histology

Recipient vessel (cranial and caudal part of the abdominal aorta) and grafted aortas were sampled individually, fixed with formalin and embedded in paraffin. Cross sections (5 μm) were stained with Verhoeff's haematoxylin and green trichrome according to the modified method [29]. Pathological alteration of the vessel wall was assessed by light microscopy. We compared our findings to the classification of atherosclerotic lesions recommended by the American Heart Association [26,30].

2.6. Immunohistochemistry

Cross sections (5 μm) of the aortae were mounted on Super Frost slides coated with (3-aminopropyl)-triethoxysilane (Sigma-Aldrich, Vienna, Austria), deparaffinised and rehydrated. Endogenous peroxidase activity was blocked with 0.6% H_2O_2 in methanol. After antigen unmasking in citrate buffer (pH 6.0) in a microwave oven, unspecific binding reactivity was blocked with normal goat serum (DakoCytomation, Glostrup, Denmark) or bovine serum albumin (Sigma-Aldrich, Vienna, Austria). The sections were incubated with the primary antibodies (Table 1) overnight at 4°C. Immunoreaction of rabbit and mouse primary antibodies was detected using the PowerVision™ Poly-HRP anti-Rabbit IgG IHC Kit (Immunovision Technologies, Daly City, CA, USA) and the Vector M.O.M. Peroxidase kit (Vector Laboratories, Burlingame, CA, USA), respectively. Immunoreaction of rat primary antibodies was detected by rat biotinylated mouse adsorbed secondary antibodies (Vector Laboratories, Burlingame, CA, USA) and the Vectastain Peroxidase Standard ABC kit (Vector Laboratories, Burlingame, CA, USA). The immunohistochemical reactions were visualised with diaminobenzidine (Sigma-Aldrich, Vienna, Austria) in 0.03% H_2O_2. All sections were counterstained with Mayer's haematoxylin, dehydrated and mounted with DPX (Fluka, Buchs, Switzerland). Sections of the small intestine of wild-type and Apo E-/- mice served as a

Figure 1. Counting points and lines. (A) Assessment of the estimated volume of the atherosclerotic lesion (*estV*) and the area fraction of the free vessel lumen (*AFFVL*) was based on counting the test points hitting the lesion (highlighted as yellow), or the lumen, respectively. The grid parameter *a* corresponds to the area of one test point. Scale bar 170 μm. (B) Circular arcs were used for estimating length density of elastin fibres and membranes. Scale bar 60 μm. Green trichrome and Verhoeff's hematoxylin stain.

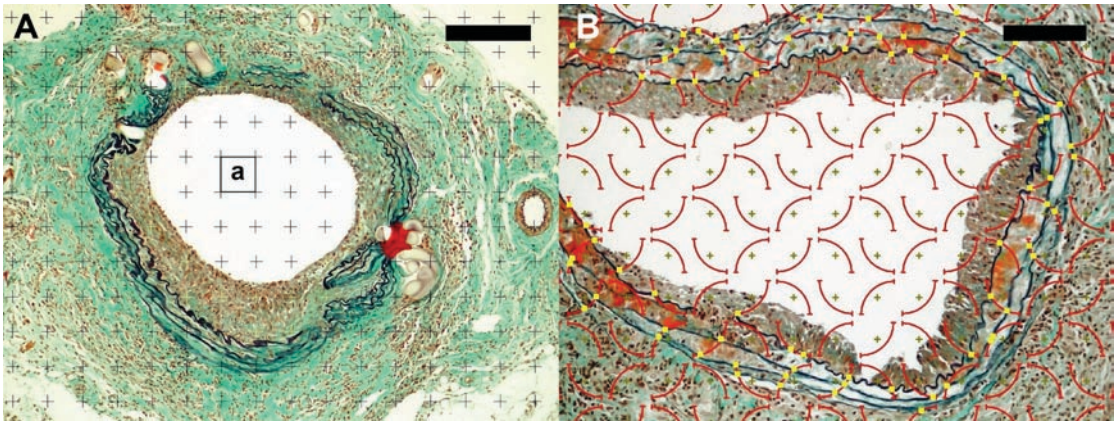

Figure 2. Analysis of sampling error. Average values of the Gundersen and Jensen's coefficient of error (*estCE(GJ)*) for all sampling combinations of corresponding values of *m* (the number of sections). The pilot study was performed for volume of both vessel lumen (avg(lumen)) and lesions (avg(lesion)). To keep the CE ≈ 0.05 for each of the parameters, the suitable value of *m*=8 was found.

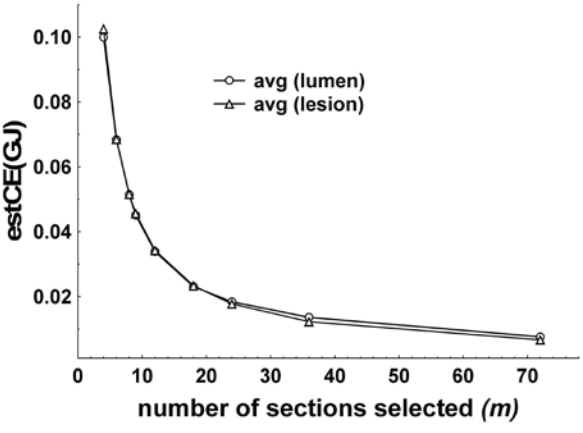

positive control. For the negative control, unspecific rat, rabbit and mouse IgG were used instead of the primary antibody.

2.7. Quantitative assessment of alterations of the vessel wall

For a quantitative analysis, we followed the well-documented methodology of [31] with respect to general principles of stereology [32]. These methods allow a reliable estimation of lesion volume in a three dimensional space. Furthermore, it is possible to assess quantitatively whether certain structures are distributed randomly or their occurrence is related to the pathological changes of the vessel under study.

In order to estimate angiostenosis and size of the atherosclerotic lesion in each sample, a segment of 0.36 mm underwent a stereological analysis with the use of the PointGrid module (Figure 1A) of the Ellipse software (ViDiTo, Kosice, Slovakia). Within the reference volume, equidistant sections were selected through systematic uniform random sampling. The position of the first tissue section in the volume was random, i.e. equal to a product of *(72*n)*, where *n* was a random number between 0 and 1. Starting with this section, every ninth section was captured with two constant magnifications so that the distance between the two neighbouring calibrated photomicrographs (sampling period) was 45 μm. We assessed the area of an atherosclerotic or arteriosclerotic lesion in each tissue section according to Equation 1:

$$estA = a \cdot P, \quad (1)$$

where *estA* was the estimated area of the arteriosclerotic lesion or of the vessel lumen, the grid parameter *a* was the area corresponding to one test point and *P* was the number of test points hitting the arteriosclerotic lesion or vessel lumen. The total number of points counted was at least 200 in all sections of each series. The Cavalieri principle [33] was used for the estimation of the volume *V* of the arteriosclerotic lesion within the reference segment of the aorta (Equation 2):

$$estV = T \cdot (A_1 + A_2 + ... + A_m), \quad (2)$$

where *estV* was the Cavalieri volume estimator, *T = 0.045 mm* was the distance between the two following selected sections, A_i was the area of the arteriosclerotic lesion or vessel lumen in the *i*-th section, and *m* stood for the total number of sections selected from the series. To estimate the value of *m,* i.e. the variation caused by sampling the serial sections, we used Gundersen and Jensen's [34] method to predict the coefficient of error (CE). Preliminary analysis proved

that the number of sections sampled within each tissue block had to be *m=8* in order to keep the CE ≈ 0.05 (Figure 2).

The relative obliteration of the aortic lumen by the arteriosclerotic lesion was characterised by the area fraction of the free vessel lumen *(AFFVL)* (Equation 3):

$$AFFVL = \left[(1 - \frac{A(lesion)}{A(lumen)}) \right] \cdot 100\%, \quad (3)$$

where *A(lesion)* was the area of the arteriosclerotic lesion, and *A(lumen)* was the area of the total vessel lumen, including the lesion. In cases of deeper invasion of the lesion towards the tunica media, where the border between the subendothelial connective tissue and tunica media was altered, the outer border of the arteriosclerotic lesion was considered to be at the level of the innermost elastic lamina.

Elastinolysis was assessed by means of the length density of profiles of elastin fibres and membranes using the relation $L_A=L/A$, where L_A was the length density of elastin fibres (intensity of planar fibre process, [35]), *L* was the estimated length of elastin profiles and *A* was the reference area the tunica media. The method (module LineSystem, software Ellipse) was based on counting the intersections of elastin fibres and membranes with a system of circular arcs randomly superposed on the micrographs (Figure 1B). The results are presented as average values for each set of 8 micrographs per tissue sample.

We tested the randomness of spatial patterns of T- and B-lymphocytes, neutrophilic granulocytes, and macrophages in sections through the vessel wall by describing the distribution of interpoint distances among the centres of gravity of the profiles of the cells [36] at the intervals 0-600 μm. The method was based on the analysis of paired correlation (clustering) and cross-correlation (colocalisation) functions implemented in the module Gold of Ellipse software. The vessel wall was selected as the region of interest, while the vessel lumen was excluded from the reference space. The same testing procedure as for clustering (local increase of density) was performed to test colocalisation of the leukocytes with the stitches. Monte Carlo estimates of two-sided 95% confidence intervals for histogram bar heights and one-sided 1% and 5% tests for clustering or colocalisation were carried out using 999 simulations of *N* realisations (*N* was equal to the number of evaluated images) of the binomial process with number of simulated points equal to the number of observed points. Similarly, calculated critical values were used for verifying the clustering and/or colocalisation of the particles: for the one-sided tests the 50th value from the maximum was used at 5% confidence level, and the 10th value from the maximum at a 1% confidence level.

2.8. Statistics

The data were processed with the Statistica Base 7.1 (StatSoft, Inc., Tulsa, OK, USA). The Shapiro-Wilks' W test was used in testing for normality. The Kruskal-Wallis test was used to compare the groups under study. The differences were considered statistically significant if $p<0.05$. The concordance between three observers was quantified with the intraclass correlation coefficient (ICC) [37]. The results of lipid analysis are presented as mean ± standard deviation.

3. Results

3.1. Animals and surgery

The basal cholesterolemia was 13.20 ± 1.64 mmol/l in the ApoE-/- mice and 2.14 ± 0.13 mmol/l in the wild-type mice. Three animals died during the operation or on the operation day due to non-patency of the aorta. Six other animals died during the first week after transplantation. The overall survival rate in the transplanted animals was 62.5%. All survivor recipients appeared to be healthy and behaved normally.

3.2. Morphology of adjacent segments of the donor aorta

The aortic segments of wild-type mice adjacent to the transplanted segment contained no lesions (Figure 3A). In several aortae of ApoE-/- mice, foam cells were found in small initial eccentric lesions comparable to human type I lesions (Figure 3B), but most of the vessels were free of any lesions, even in the regions of arterial branching. Immunohistochemistry proved only occasional lymphocytes and neutrophils (but no macrophages) in the vicinity of the vasa vasorum. No difference between the proximal (upstream) and distal (downstream) non-transplanted segments was found.

3.3. Morphology of aortic grafts

In all groups, transplantation led to neointima formation (Figure 3C) as well as disruption and regression of the elastic lamellae (Figure 3D) in the tunica media of the grafted aorta. The neointima was rich in smooth muscle cells. In Group 1, where ApoE-/- were donors as well as recipients, initial type I lesions were found, but without any qualitative difference when compared to the non-transplanted segments.

In all the transplanted aorta segments, i.e. in samples from Groups 1, 2, and 3, the endothelium was continuous. No signs of neoangiogenesis within the intima were observed. In some cases, the part of the adventitia facing the stitch was slightly thickened with

Figure 3. Histology of aorta grafts and adjacent host aorta segments. (A) Non-transplanted lesion-free abdominal aorta of a wild-type mouse (Group 3). Scale bar 100 μm. (B) Foam cells in the intima of an ApoE-/- mouse, non-transplanted segment (Group 1). Scale bar 50 μm. (C) Aorta of a wild-typeto wild-typetransplantation case (Group 3) with nearly concentric intimal thickening. Scale bar 200 mm. (D) Same, detail of elastinolysis and inflammatory cells surrounding the stitch. Scale bar 50 μm. A-D were stained with green trichrome and Verhoeff's hematoxylin. (E) T-lymphocytes infiltrating the tunica media of a transplanted aorta segment of a wild-type mouse (Group 3), immunohistochemical detection of CD3. Scale bar 50 μm. (F) B-lymphocytes surrounding the stitch in the tunica adventitia of a transplanted aorta segment of an ApoE-/- mouse (Group 2), immunohistochemical detection of CD20. Scale bar 70 mm. (G) Macrophages in the tunica adventitia of the same sample as in F, immunohistochemical detection of MCA 874G. Scale bar 70 μm. (H) Neutrophilic leukocytes encircle a stitch in the tunica adventitia of a transplanted segment of an ApoE-/- mouse (Group 1), immunohistochemical detection using an anti-mouse neutrophils antibody. Scale bar 100 mm. (E-H) Visualisation of the immunoreaction horseradish peroxidase/diaminobenzidine.

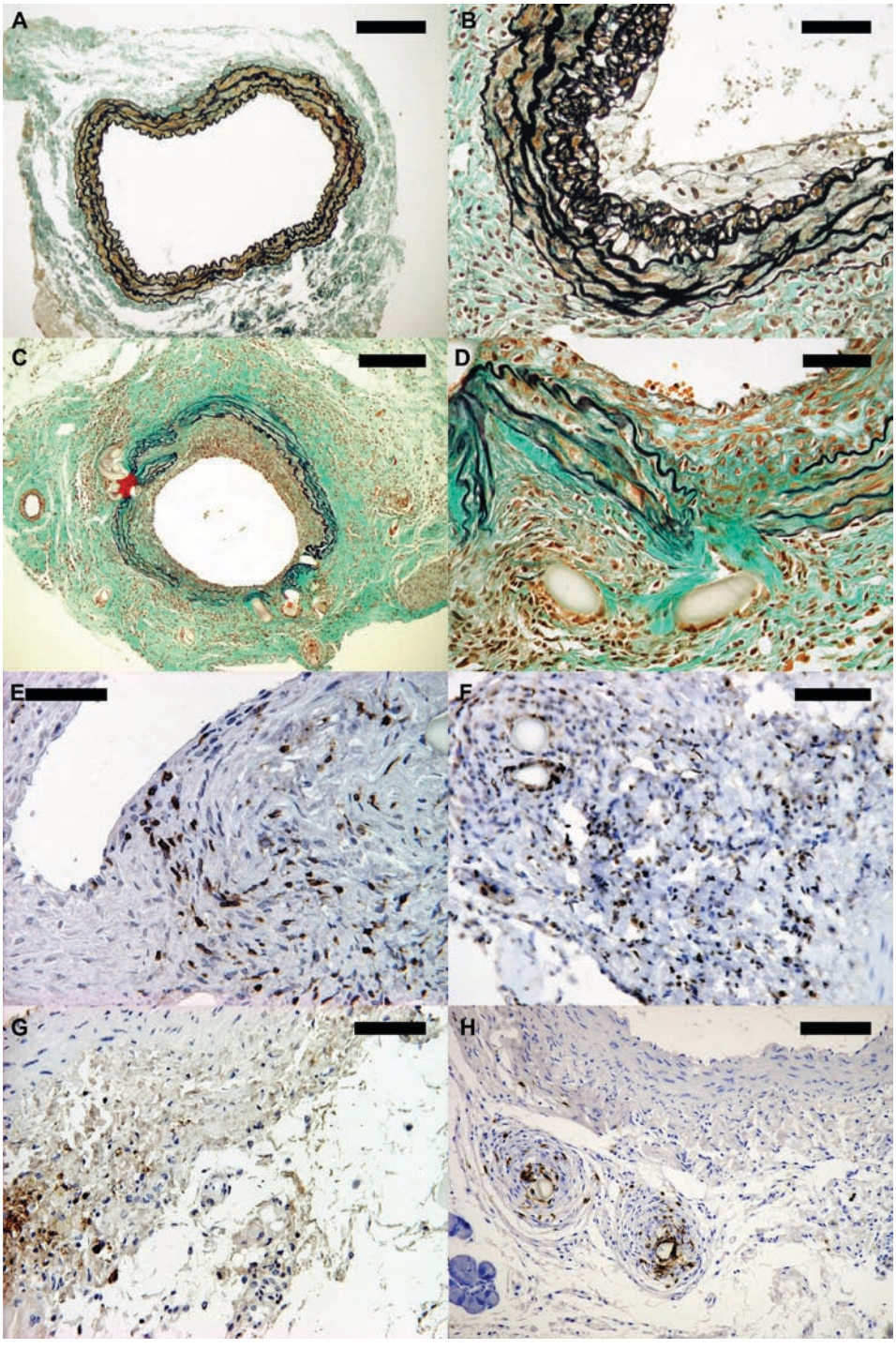

Table 2. Spatial distribution of leukocytes within the transplanted aortic grafts.

	Clustering in the intervals: [μm]		Colocalisation with stitches in the intervals: [μm]	
	$p<0.01$	$0.01<p<0.05$	$p<0.01$	$0.01<p<0.05$
T-lymphocytes	10-150	none	100-150	80-100, 150-200
B-lymphocytes	10-80	none	10-50, 60-70	70-80
Macrophages	10-150	none	10-40	none
Neutrophilic leukocytes	10-90	none	20-30, 40-50	30-40,50-60

increased cellularity in comparison with the other parts of the adventitia. In this region, neutrophilic granulocytes and T-lymphocytes were found. In two specimens, only T-lymphocytes invaded the tunica media of the aorta (Figure 3E). In some cases, an increased amount of connective tissue was present in the adventitia next to the stitches. T- and B-lymphocytes (Figure 3E, 3F), a few macrophages (Figure 3G) and neutrophils (Figure 3H) were found in this location, dispersed among collagen fibres and fibrocytes. The stitches were usually encircled by a capsule composed of concentrically arranged fusiform cells. This capsule contained a large number of neutrophilic granulocytes with normal nuclei and B-lymphocytes.

3.4. Quantification of lesions after transplantation

The *estV* of the lesion, *AFFVL* and elastin length density did not differ between the individual groups of this study (Figure 4). However, in all the transplanted grafts of the aorta *estV* of the lesion was higher *($p<0.001$)*, the *AFFVL* and the elastin length density were lower *($p<0.001$* for both*)* than in neighbouring proximal and distal non-transplanted segments. The Pearson correlation coefficient between *estV* and *AFFVL* was -0.41, between *estV* and L_A it was 0.36, and between *AFFVL* and L_A it was 0.63. Seven samples were excluded from quantification because of mechanical damage to the vessel wall, which did not allow reliable morphometry. The variability among three independent observers in estimates of lesion volume and length density of elastin network is presented in Figure 5 as values of the intraclass correlation coefficient.

3.5. Spatial distribution of leukocytes

In transplanted grafts, all types of leukocytes, i.e. lymphocytes, monocytes/macrophages and neutrophilic granulocytes, were arranged in significant non-random clusters, which were colocalised with stitches within the intervals summarised in Table 2.

4. Discussion

4.1. Clinical outcome

Although Chereshnev et al. [20] reported excellent results with a 100% recovering rate in 26-week-old animals, other findings [18,19] with 70-80% success seem much more likely and correspond to the survival rate in our study (62.5%). When developing a mouse aortic transplantation model, Koulack et al. [28] reported an initial 75% mortality rate (caused mainly by thrombosis and shock), which was improved to a success rate of >80% after performing nearly 200 operations. As our experiment was carefully performed by a skilled technician with sufficient experience in microsurgery on small laboratory animals, the present results cast doubt on the reproducibility of the transplantation model of atherosclerosis regression in young mice. The surgery might have coincided with the normal growth of aorta so the alteration of the vessel wall by invasive procedure and damage to the nervi and vasa vasorum resulted in much more pronounced formation of concentric neointima rich in smooth muscle cells than known from adult animals. With the exception of age, no other factor exists which might explain the relatively high mortality and significant transplant arteriosclerosis in young animals used in this study.

4.2. Lesions in the transplanted aorta sections and transplant arteriosclerosis

Structural alterations observed in transplanted aorta sections in comparison with host aorta segments included development and/or increasing volume of the arteriosclerotic lesion, decrease of the free vessel lumen, neointima formation, elastinolysis and accumulation of immune cells in the vessel wall.

The volume of the arteriosclerotic lesions as well as the decrease of the free vessel lumen in the transplanted aorta segment strikingly did not differ between the individual study groups (Figure 4A-D). Although the median of *estV* of the lesions was higher in Group 1, i.e., in ApoE-/- recipients, than in the other groups with wild-type recipients, the difference was not significant.

Figure 4. Quantitative analysis of aortae in the experimental groups and in samples taken from different sites. (A, B) Estimated volume of lesions (*estV*), (C, D) area fraction of the free vessel lumen (*AFFVL*), and (E, F) length density (L_A) of elastin fibres. Values are medians with 25-75 percentiles, n=12 in Group 1 (ApoE-/- to ApoE-/-), n=13 in Group 2 (ApoE-/- to wild-type(WT)), n=13 in Group 3 (WT to WT), n=12 in *transplanted*, n=12 in *proximal*, n=13 in *distal*. P-values of Kruskal-Wallis ANOVA are presented, *n.s.* – non significant. *Proximal* and *distal* are non-transplanted aortic segments adjacent to the *transplanted* graft.

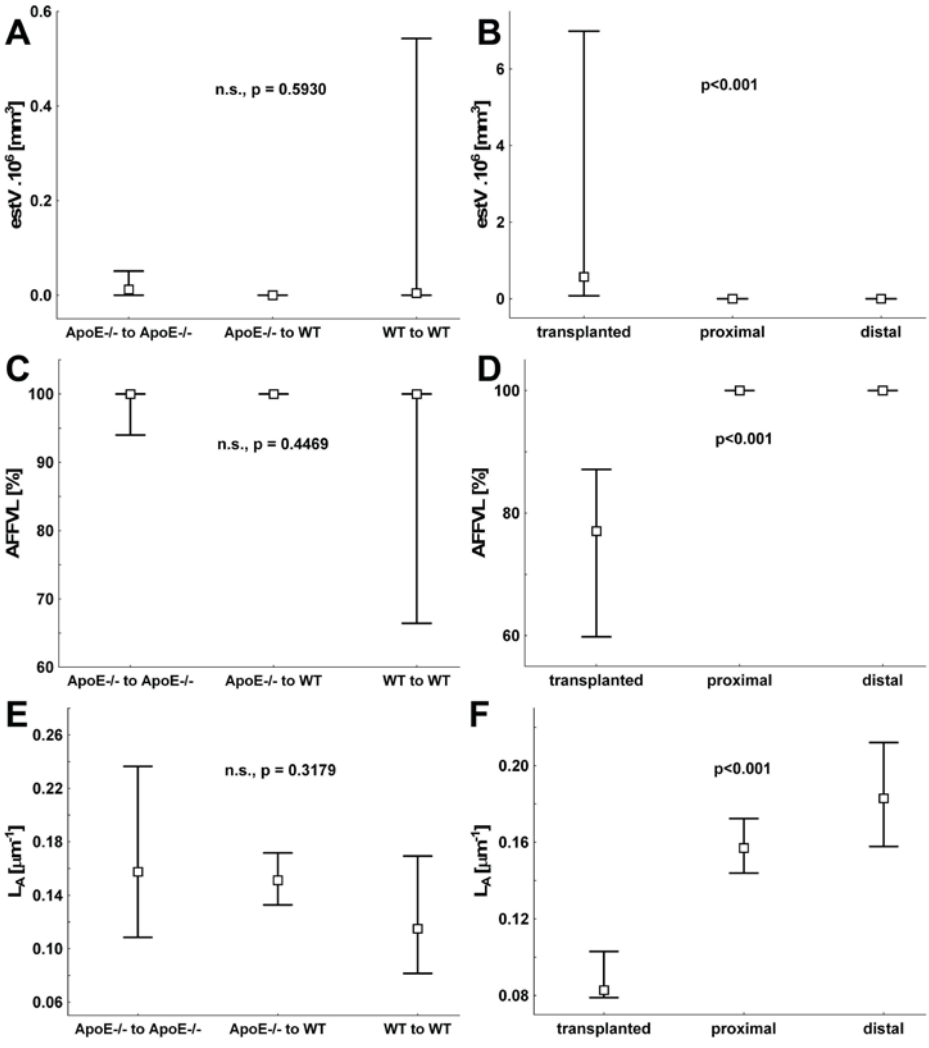

Fatty streak formation did not occur or progress in any of the analysed samples. Since Lee et al. [38] reported about the protective role of nitric oxide synthase (NOS) induced by aortic transplantation, we speculate that NOS might have inhibited adhesion of leukocytes and further progression of initial fatty streaks in all transplanted specimens, thus compensating the hyperlipidemia in ApoE-/- mouse.

The lesions found in transplanted specimens have probably to be considered as transplant arteriopathy rather than progression of initial atherosclerotic lesions. The etiology of transplant arteriosclerosis was suggested to be multifactorial and its precise mechanism to date remains obscure [39]. In the rat, the severity of age-related neointima formation in syngeneic aorta transplantation (in the absence of alloreactivity and immunosuppressive drugs) is primarily determined by the recipient's age rather than the donor's age, with young recipients generally being less affected [40]. This complies with the fact that the lowest *AFFVL* in juvenile ApoE-/- mice was 60%, i.e. the narrowing of the vessel lumen caused by transplant arteriosclerosis was far from being occlusive, perhaps due to the known arterioprotective property of bone marrow-derived progenitor cells in juvenile ApoE-/- mice [41].

Neointima formation in our experiment was qualitatively the same as usually reported from allograft studies in mice [42,43]. However, as neointima proliferation, endothelial regeneration [44], and smooth muscle cells recruitment are dependent on alloimmune cellular responses [42] and involvement of hematopoietic stem cells [45], we have no evidence showing that the

Figure 5. Intraclass correlation coefficients (ICC). The variability among three independent observers in estimates of lesion volume and of length density of elastin network. Values are ICC and lower-upper limits of the 95% confidence intervals.

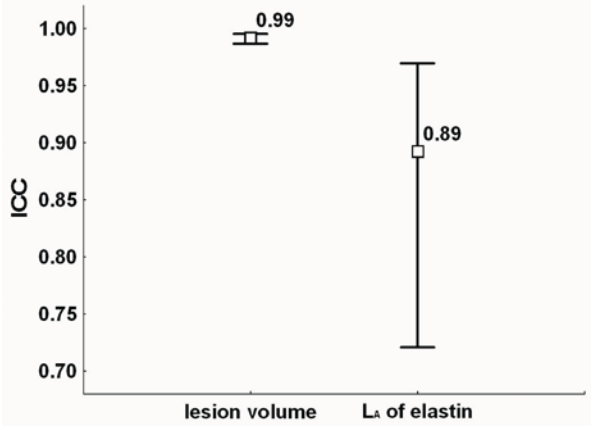

mechanisms of transplant arteriosclerosis are the same in syngeneic as in non-syngeneic transplantation. Detailed descriptions of transplant arteriosclerosis in syngeneic aortic transplantation in mice are not available. We can only speculate that our findings suggest that the susceptibility to transplant arteriosclerosis might be higher in ApoE-/- mice than in female Fisher rats [40], where neointimal lesions after syngeneic transplantation could not be detected. To elucidate these questions, a detailed study focused on transplant arteriosclerosis in syngeneic mice would be required, e.g. quantitative immunohistochemistry of adhesion molecules (VCAM, ICAM), electron microscopy to reveal the phenotypic alteration of vascular smooth muscle cells, assessment of kinetics of cytokine production and MHC-matching. Such results would be comparable to those [46], who performed their studies on partially and fully allogeneic mouse.

Elastin degradation is generally related to advanced atherosclerotic lesions rich in macrophage-borne proteases, but not to initial atherosclerotic lesions [47]. Since we found only slight arteriosclerotic lesions (type I) but significant elastinolysis, we conclude that atherosclerosis itself did not contribute to the decrease of elastin length density. Elastin destruction observed in transplanted specimen corresponded to the distribution pattern of macrophages which surrounded the stitches. At these sites, elastinolysis was also most evident. Degradation of elastin fibres, accumulation of immune cells and fibrous encapsulation of the stitches probably represent rather stages of healing processes than an answer to infection during surgery, since neither bacteria nor neutrophilic granulocytes with hypersegmented nuclei could be found.

4.3. Histological quantification in assessment of development and regression of atherosclerotic lesions

Based on our experience, stereology provided us with reproducible quantitative estimates, which were achieved with a reasonable effort. The sampling strategy used for the Cavalieri method was based on systematic uniform random sampling, the variability of which was low enough. Point counting method seemed to be more laborious but more robust to the staining variation than the segmentation methods used for the same purpose [19]. As the lower limits of the 95% confidence intervals of the intraclass correlation coefficient exceeded 0.7 in both *estV* of atherosclerotic lesions and length density of the elastic fibres, we consider the interobserver variability to be low enough. The wider confidence intervals in the length density of elastin fibres was caused by successive branching of the main elastin fibres into a fine network so that the very detailed demarcation of the delicate fibres remained rather subjective. The *AFFVL* parameter and *estV* of arteriosclerotic lesions must be considered as complementary. The *AFFVL* parameter is relatively robust with respect to the deviation of the section plane in regard to the transversal plane. In spite of the careful orientation of the paraffin-embedded tissue sample, the chance of a deviation occurring cannot be entirely excluded. As *AFFVL* is a dimensionless ratio, it does not become biased by absolute differences in the size or shape of the aorta among the animals; it was used as an obstruction measure of the lumen by the lesion. Taking into account the size of the reference volume, it becomes apparent that, in most cases, we assessed the size of one lesion rather than several lesions. According to our experience, stereological assessment has proven to be accurate, correct and reproducible. If the bias of the results caused by the irregular shape of the lesion were avoided, the total number of test points hitting the area of interest should be above 80. This number was estimated according to the nomogram of Gundersen and Jensen [34], which took into account the irregular shape of the lesion and a *CE<0.05* for the estimate. In our method, this conventional limit was certainly exceeded, ranging from 200 to 300 intersections (depending on both lumen and lesion shape and size).

We conclude that no regression of initial atherosclerotic lesion was achieved by syngeneic heterotopic transplantation of thoracic aorta segments of young ApoE-/- mice to wild-type recipients of the same age. On the contrary, neointima formation, arteriosclerosis and degradation of elastin prevailed in all transplanted specimens, even in control groups. It is suggested that the tiny, sensitive walls of young aorta suffered from

severe disturbance of the vasa and nervi vasorum caused by the invasive intervention in the transplanted animals, so that it became vulnerable to inflammation and transplant arteriopathy. The reproducibility of the promising regression model in 12-week-old mice was derogated by the striking dependence of the results upon the operation technique. Thoracic to abdominal aorta transplantation did not offer a method which would enable us to study atherosclerosis regression in 12-week-old Apo E-/- mice. Stereological assessment not only proved to be accurate, correct and reproducible but also provided us with with robust quantitative estimates achieved with a reasonable effort.

Acknowledgements

The experimental part of the work was supported by the grant 1M6798582302, and the histological evaluation was supported by the project MSM0021620819 and MSM4977751303, all of them awarded by the Ministry of Education, Youth and Sports of the Czech Republic. The cooperation among the authors received support from The Scientific cooperation between Czech Republic and Austria, Project Kontakt ME09090. Special thanks to Mrs. Magdalena Helmreich (Vienna, Austria) for performing the immunohistochemical processing.

References

[1] Plump A.S., Smith J.D., Hayek T., Aalto-Setala K., Walsh A., Verstuyft J.G., Rubin E.M., Breslow J.L. Severe hypercholesterolemia and atherosclerosis in apolipoprotein E- deficient mice created by homologous recombination in ES cells. Cell, 1992, 71,343-353

[2] Breslow J.L. Transgenic mouse model of lipoprotein metabolism and atherosclerosis. PNAS, 1993, 90, 8314-8318

[3] Breslow J.L. Mouse models of atherosclerosis. Science 1996, 272, 685-688

[4] von Eckardstein A. Cholesterol efflux from macrophages and other cells. Curr. Opin. Lipidol., 1996, 7, 308-319

[5] Curtiss L.K. ApoE in atherosclerosis: A protein with multiple hats. Arterioscler. Thromb. Vasc. Biol., 2000, 20, 1852-1853

[6] Greenow K., Pearce N.J., Ramji D.P. The key role of apolipoprotein E in atherosclerosis. J. Mol. Med., 2005, 83, 329-342.

[7] van Ree J.H., van den Broek W.J., Dahlmans V.E., Groot P.H., Vidgeon-Hart M., Frants R.R., Wieringa B., Havekes L.M., Hofker M.H. Diet-induced hypercholesterolemia and atherosclerosis in heterozygous apolipoprotein E-deficient mice. Atherosclerosis, 1994, 111, 25-37

[8] Nakashima Y., Plump A.S., Raines E.W., Breslow J.L., Ross R. ApoE-deficient mice develop lesions of all phases of atherosclerosis throughout the arterial tree. Arterioscler. Thromb. Vasc. Biol., 1994, 14, 133-140

[9] Jawien J., Nastalek P., Korbut R. Mouse models of experimental atherosclerosis. J. Physiol. Pharmacol., 2004, 55, 503-517

[10] Ohashi R., Mu H., Yao Q., Chen C. Cellular and molecular mechanisms of atherosclerosis with mouse models. Trends Cardiovasc. Med., 2004, 14, 187-190

[11] Garber D.W., Kulkarni K.R., Anantharamaiah G.M. A sensitive and convenient method for lipoprotein profile analysis of individual mouse plasma samples. J. Lip. Res., 2000, 41, 1020-1026

[12] Havel R.J., Eder H.A., Bragdon J.H. The distribution and chemical composition of ultracentrifugally separated lipoproteins in human serum. J. Clin. Invest., 1955, 34, 1345-1353

[13] Gotto A.M. Jr., Pownall H.J., Havel R.J. Introduction to the Plasma Lipoproteins. In: Segrest J.P., Albers J.J. (Eds.), Methods in Enzymology, Vol. 128. Plasma Lipoproteins. Part A. Preparation, Structure, and Molecular Biology Academic Press, Orlando, 1986

[14] Shi W., Wang X,, Wang N.J., McBride W.H., Lusis A.J. Effect of macrophage-derived apolipoprotein E on established atherosclerosis in apolipoprotein E-deficient mice. Arterioscler. Thromb. Vasc. Biol., 2000, 20, 2261-2266

[15] van Eck M., Herijgers N., van Dijk K.W., Havekes L.M., Hofker M.H., Groot P.H., van Berkel T.J. Effect of macrophage-derived mouse ApoE, human ApoE3-Leiden, and human ApoE2, (Arg158->Cys) on cholesterol levels and atherosclerosis in ApoE-deficient mice. Arterioscler. Thromb. Vasc. Biol., 2000, 20, 119-127

[16] Gough P.J., Raines E.W. Gene therapy of apolipoprotein E-deficient mice using a novel macrophage-specific retroviral vector. Blood, 2003, 101, 485-491

[17] Su Y.R., Ishiguro H., Major A.S., Dove D.E., Zhang W., Hasty A.H., Babaev V.R., Linton M.F., Fazio S. Macrophage apolipoprotein A-I expression protects against atherosclerosis in ApoE-deficient mice and up-regulates ABC transporters. Mol. Ther., 2003, 8, 576-583

[18] Reis E.D., Li J., Fayad Z.A., Rong J.X., Hansoty D., Aguinaldo J.G., Fallon J.T., Fisher E.A. Dramatic remodeling of advanced atherosclerotic plaques of the apolipoprotein E-deficient mouse in a novel transplantation model. J. Vasc. Surg., 2001, 34, 541-547

[19] Rong J.X., Li J., Reis E.D., Choudhury R.P., Dansky H.M., Elmalem V.I., Fallon J.T., Breslow J.L., Fisher E.A. Elevating high-density lipoprotein cholesterol in apolipoprotein E - deficient mice remodels advanced atherosclerotic lesions by decreasing macrophage and increasing smooth muscle cell content. Circulation, 2001, 104, 2447-2452

[20] Chereshnev I., Trogan E., Omerhodzic S., Itskovich V., Aguinaldo J.G., Fayad Z.A., Fisher E.A., Reis E.D. Mouse model of heterotopic aortic arch transplantation. J. Surg. Res., 2003, 111, 171-176

[21] Trogan E., Fayad Z.A., Itskovich V.V., Aguinaldo J.G., Mani V., Fallon J.T., Chereshnev I., Fisher E.A. Serial studies of mouse atherosclerosis by in vivo magnetic resonance imaging detect lesion regression after correction of dyslipidemia. Arterioscler. Thromb. Vasc. Biol., 2004, 24, 1714-1719

[22] Hansson G.K. Immune mechanisms in atherosclerosis. Arterioscler. Thromb. Vasc. Biol., 2001, 21, 1876-1890

[23] Libby P. Inflammation in atherosclerosis. Nature, 2002, 420, 868-874

[24] Boyle J.J. Macrophage activation in atherosclerosis: Pathogenesis and pharmacology of plaque rupture. Curr. Vasc. Pharmacol., 2005, 3, 63-68

[25] Moos M.P.W., John N., Gräbner R., Nossmann S., Gunther B., Vollandt R., Funk C.D., Kaiser B., Habenicht A.J. The lamina adventitia is the major site of immune cell accumulation in standard chow-fed apolipoprotein E-deficient mice. Arterioscler. Thromb. Vasc. Biol., 2005, 25, 2386-2391

[26] Tonar Z., Bobkova D., Havlickova J., Poledne R. Vessel transplantation of apolipoprotein E-deficient mice as a model of atherosclerosis regression. Atherosclerosis Suppl., 2005, 6, 45-45

[27] European Communities. European convention for the protection of vertebrate animals used for experimental and other scientific purposes. 1986, European Treaty Series No. 123, Strasbourg

[28] Koulack J., McAlister V.C., Giacomantonio C.A., Bitter-Suermann H, MacDonald A.S., Lee T.D. Development of a mouse aortic transplant model of chronic rejection. Microsurgery, 1995, 16, 110-113

[29] Kocova J. Overall staining of connective tissue and the muscular layer of vessels. Fol. Morphol., 1970, 3, 293-295

[30] Stary H.C. Natural History and Histological Classification of Atherosclerotic Lesions. An Update. Arterioscler. Thromb. Vasc. Biol., 2000, 20, 1177-1178

[31] Nachtigal P., Semecky V., Kopecky M., Gojova A., Solichova D., Zdansky P., Zadak Z. Application of stereological methods for the quantification of VCAM-1and ICAM-1 expression in early stages of rabbit atherosclerosis. Pathol. Res. Pract., 2004, 200, 219-229

[32] Howard C.V., Reed M.G. Unbiased Stereology: Three Dimensional Measurement in Microscopy. 1st edn. Royal Microscopical Society and Springer-Verlag, New York, 1998.

[33] Russ J.C., Dehoff R.T. Classical stereological measures. In: Russ J.C., Dehoff R.T. (Eds). Practical Stereology. 2nd edn. Plenum Press, New York, 2001

[34] Gundersen H.J.G., Jensen E.B. The efficiency of systematic sampling in stereology and its prediction. J. Microsc., 1987, 147, 229-263

[35] Stoyan D., Kendall W.S., Mecke J. Fibre and surface processes. In: Stoyan, D, Kendall, WS, Mecke, J (Eds). Stochastic geometry and its applications. 2nd edn. John Wiley & Sons, Chichester, 1996

[36] Philimonenko A.A., Janacek J., Hozak P. Statistical evaluation of colocalisation patterns in immunogold labelling experiments. J. Struct. Biol., 2000, 132, 201-210

[37] Shrout P.E., Fleiss J.L. Intraclass Correlations: Uses in Assessing Rater Reliability. Psych. Bull., 1979, 2, 420-428

[38] Lee P.C., Wang Z.L., Qian S., Watkins S.C., Lizonova A., Kovesdi I., Tzeng E., Simmons R.L., Billiar T.R., Shears L.L. Endothelial nitric oxide synthase protects aortic allografts from the development of transplant arteriosclerosis. Transplantation, 2000, 69, 1186-1192

[39] Soleimani B., Shi V.C. Experimental models of graft arteriosclerosis. Methods Mol. Biol., 2006, 333, 401-424

[40] Calfa M., Aitouche A., Vazquez-Padron R.I., Gay-Rabinstein C., Lasko D., Badell J., Farji A., El-Haddad A., Liotta C., Louis L.B., Simmonds A., Pestana I.A., Pang M., Li S., Pham S.M. Aging and transplant arteriosclerosis in absence of alloreactivity and immunosuppressive drugs in a rat aortic model: recipient age's contribution. Transplantation, 2005, 79, 1683-1690

[41] Rauscher F.M., Goldschmidt-Clermont P.J., Davis B.H., Wang T., Gregg D., Ramaswami P., Pippen A.M., Annex B.H., Dong C., Taylor D.A. Aging, progenitor cell exhaustion, and atherosclerosis.

Circulation, 2003, 29, 457-463
[42] Chow L.H., Huh S., Jiang J., Zhong R., Pickering J.G. Intimal thickening develops without humoral immunity in a mouse aortic allograft model of chronic vascular rejection. Circulation, 1996, 94, 3079-3082
[43] Sun H., Valdivia L.A., Subbotin V. Improved surgical technique for the establishment of a murine model of aortic transplantation. Microsurgery, 1998, 18, 368-371
[44] Hu Y., Davison F., Zhang Z., Xu Q. Endothelial replacement and angiogenesis in arteriosclerotic lesions of allografts are contributed by circulating progenitor cells. Circulation, 2003, 108, 3122-3127
[45] Sakihama H., Masunaga T., Yamashita K., Hashimoto T., Inobe M., Todo S., Uede T. Stromal cell-derived factor-1 and CXCR4 interaction is critical for development of transplant arteriosclerosis. Circulation, 2004, 110, 2924-2930
[46] Gough P.J., Gomez I.G., Wille P.T., Raines E.W. Macrophage expression of active MMP-9 induces acute plaque disruption in apoE-deficient mice. Journal Clin. Invest., 2006, 116, 59-69
[47] Ensminger S.M., Spriewald B.M., Witzke O., Morrison K., Pajaro O.E., Morris P.J., Rose M.L., Wood K.J. Kinetics of transplant arteriosclerosis in MHC-class I mismatched and fully allogeneic mouse aortic allografts, Transplantation, 2002, 73, 1068-1074